Int. J. Heat Mass Transfer. Vol. 29, No. 1, pp. 1–19, 1986
Printed in Great Britain

0017–9310/86 $3.00 + 0.00
Pergamon Press Ltd.

Determination of the time-resolved probabilities of heterogeneous recombination of atoms in shock tube experiments

V. D. BERKUT, V. V. KOVTUN, N. N. KUDRYAVTSEV, S. S. NOVIKOV and A. I. SHAROVATOV

Institute of Chemical Physics of the USSR Academy of Sciences, 117977 Moscow, U.S.S.R.

(*Received* 6 *August* 1984)

Abstract—A technique is devised and implemented experimentally for measuring time-resolved probabilities of heterogeneous surface recombination of atoms on a plate with a sharp leading edge exposed to a pulsing supersonic flow of gas dissociated by an incident shock wave propagating in a shock tube. A method to calculate heat transfer on the plate surface for the conditions pertaining to the experiment is suggested. The design of a heat flux gauge and the technology of its fabrication are developed.

1. INTRODUCTION

RECOMBINATION catalytic activity of materials interacting with a supersonic multi-component dissociated gas flow constitutes a very topical, rapidly developing branch of chemical physics which occupies a definite position at the juncture of the physics of elementary atomic–molecular processes and hypersonic aerodynamics. The interest in the studies in this field is engendered by the determining effect of heterogeneous recombination on the course of a number of physical processes in different areas of modern science and technology. Thus, when bodies move at hypersonic velocities in a rarefied gas, a substantial part of heat flux to a surface, up to 50% is due to heterogeneous atom recombination [1]. In chemical lasers with sub- and supersonic active medium flow, in sub- and supersonic chemical and plasmachemical reactors, etc., heterogeneous processes of the death of active centers, including the atomic species, exert important influence on the course of chain chemical reactions and on the operation of these devices in general.

Investigations of heterogeneous atom recombination date from the fundamental works of Roguinsky [2], Semyonov and Goldansky [3], Voyevodsky [4], Talrose [5], Smith [6], and Laverenko [7]. These workers developed original methods of studying heterogeneous atom recombination when the surface interacts with a stationary or slowly moving (at about 1 m s^{-1}) dissociated low-density gas. The probabilities of heterogeneous recombination γ_w were obtained for a number of materials, including metals and their oxides and also glass, quartz and other dielectrics, and also the orders of the surface recombination reactions were determined. An important result of these investigations is the discovery that γ_w is a function of the temperature T_w.

The influence of the parameters of a gas, interacting with the surface, on the probability of heterogeneous atom recombination has not as yet been studied adequately. Therefore, the surface recombination is investigated and the value of γ_w is measured in the conditions which correspond to the subsequent practical use of the results obtained. The demands for heat transfer calculations in the hypersonic aerodynamics, development and optimization of operating conditions of a vast number of devices employing supersonic gas flows were responsible for the development, in the last few years, of principally new laboratory methods of studying heterogeneous atom recombination on the surfaces of models in supersonic dissociated gas flow.

In laboratory modelling of multi-component dissociated gas flow interaction with surfaces a wide use is made of the steady-state blowing of a model in a plasma generator [8–13]. The shock tube technique made it possible to measure the homogeneous reaction rate constant for oxygen recombination in the wide region of high temperatures [14]. The use of shock tubes (ST) to produce pulsed supersonic flow of a thermally dissociated gas enables the elimination of the effect of metastable particles such as of the singlet oxygen $O_2^1\Delta_g$ formed in a plasma generator discharge and of the change in the chemical composition of the surface studied on the results of measurements of the heterogeneous recombination probability (catalytic activity coefficient) γ_w. An important feature of the method is the possiblity of determining time-resolved values of the heterogeneous recombination probability on surfaces that have experienced certain physicochemical effects.

The feasibility of determining the heterogeneous recombination probability by placing a model in a pulsed supersonic flow of gas dissociated by an incident shock wave propagating in a shock tube has been established in principle in refs. [15–17]. In this work the theory of the method is developed, its experimental implementation is shown and some results of

NOMENCLATURE

c_i mass concentration of components, ρ_i/ρ
C_p, C_v specific heats at constant pressure and volume, respectively
D_{ik} binary diffusion coefficient
f reduced stream function, $\Psi/\sqrt{2\xi}$
h_D specific enthalpy of gas dissociation
g dimensionless 'frozen' gas enthalpy, h_f/h_{fe}
h specific gas enthalpy, $\sum c_i h_i$
h_i specific enthalpy of mixture ith species, $\int_0^T C_{pi}\,dT + h_i^0$
h_i^0 enthalpy of ith species formation
h_{fi} specific 'frozen' gas enthalpy, $\int_0^T C_{pi}\,dT$
h_t specific total enthalpy of gas, $h + \frac{u^2}{2}$
J_i diffusion flux of ith species
K_r gas-phase reaction rate constant
K_w heterogeneous recombination rate constant
Le Lewis–Semyonov number, $\rho D_{13} C_p/\lambda$
l $\rho\mu/\rho_e\mu_e$
l_m maximum length of hot gas region
m_i molecular weight of ith species
m molecular weight of gas
M Mach number
P pressure
Pr Prandtl number, $\mu C_p/\lambda$
Q_c convection heat flux component
Q_r recombination heat flux component
Q_{wt} total heat flux to a surface
R universal gas constant
R_T shock tube radius
Sc Schmidt number, $\mu/\rho D_{13}$
T temperature
u tangential gas velocity
v normal gas velocity
x streamwise coordinate along a plate
x_i mole fraction of mixture ith species (in Appendix)
x_m distance from shock tube orifice to the section under observation
W ratio of densities across shock wave front, ρ_2/ρ_1
y transverse coordinate
z dimensionless concentration of oxygen atoms, c_i/c_{ie}.

Greek symbols

β accommodation coefficient for dissociation energy at a surface
ζ_g Damkohler number for reaction in gas phase
ζ_w Damkohler number for surface reactions
η, ξ Dorodnitsyn–Lees variables
θ expansion angle of plate in supersonic flow
κ specific heat ratio, C_p/C_v
λ thermal conductivity of gas
μ gas viscosity
$\nu(M)$ Prandtl–Meyer function
ρ gas density
τ_c chemical relaxation time behind shock wave
τ_d characteristic time of atom diffusion through boundary layer
τ_{st} lifetime of hot gas region
$\Delta\tau_{exp}$ existence of quasi-steady conditions in hot gas region (times τ_c, τ_{st} and $\Delta\tau_{exp}$ are given in a laboratory coordinate system)
τ_r characteristic time of bulk recombination in boundary layer
$\Omega_{ii}^{(1,1)*}, \Omega_{ik}^{(2,2)*}$ reduced collision integrals
σ particle collision diameter
Ψ stream function.

Subscripts

e value at boundary-layer edge
f frozen values
i, k referring to mixture components ($i, k = 1$, oxygen atoms; $i, k = 2$, oxygen molecules; $i, k = 2$, inert diluent)
s values at shock wave front
w value on body surface
1 initial gas state in shock tube
2 value of gas parameters behind shock wave.

measurements of the probability of oxygen atom recombination on silicon monoxide, platinum and alumina are presented.

The reliable recovery of the quantity γ_w can be accomplished provided that in the conditions pertaining to the experiment the recombination heat flux constitutes a considerable portion of the total heat flux to the surface. The second necessary condition is the provision of the possibility for the highly accurate prediction of the state of the gas interacting with the surface and, consequently, for theoretical recovery of the recombination and conduction heat fluxes.

In the present work it is suggested that the value of γ_w be determined by comparing the measured and calculated heat fluxes to the gauge in the form of a flat

plate, with a sharp leading edge, placed parallel, or at a small expansion angle, to the gas flow. The supersonic flow of a dissociated gas is realized downstream of an incident shock wave (SW) propagating in a shock tube and provides a quasi-steady-state regime of flow past a plate lasting 100–200 μs. Heat fluxes are measured by a thin-film resistance thermometer located some distance upstream from the plate leading edge. The substance investigated, in the form of a narrow band, is vacuum deposited over the resistance thermometer on top of a layer of insulating material. It is shown that the method extends the gas pressures studied by about two orders of magnitude—up to about 100 mmHg.

2. THE CHOICE OF THE SHOCK TUBE OPERATING CONDITIONS

The heat flux due to heterogeneous atom recombination attains its maximum values in the case of the absence of gas-phase recombination of atoms, i.e. when the boundary layer near the model is a chemically 'frozen' one. In order that the fraction of atoms that recombine in the gas phase should not be more than several per cent, it is necessary that the gas phase Damkohler number, $\zeta_g = \tau_g/\tau_r$, should be less than 10^{-3}–10^{-4} [18]. For a laminar boundary layer on a flat plate the calculation of the characteristic times τ_d and τ_r yields the following relation for ζ_g [18]

$$\zeta_g = \frac{4x}{u_e}\cdot\frac{2K_r(T_e)}{T_e^2}\cdot\left(\frac{P_e}{R}\right)^2 \qquad (1)$$

where K_r is the gas-phase recombination rate constant (Table 1, reaction 7), u_e, T_e and P_e are the velocity, temperature and pressure of the gas at the boundary-layer edge, x is the distance to the plate leading edge. The required dissociation degree for O_2 molecules is achieved at the temperatures $T_e \simeq 3500$–4000 K corresponding to $u_e \simeq (3\text{–}5)\times 10^5$ cm s^{-1}. For the characteristic dimensions of the model, $x = 1$ cm, it follows from equation (1) that the pressure P_e at the boundary layer edge should not exceed 200–250 mmHg.

The complete dissociation of molecular oxygen required to provide the maximum portion of the recombination heat flux is achieved at the incident SW Mach numbers $M_s = 10$–18. Taking into account the requirement that chemical reactions in the boundary layer should be frozen leads to the limitation on the mixture initial pressure in the shock tube, e.g. that $P_1 \lesssim 1.0$–2.0 mmHg.

The shock tube operation at low initial pressures, $P_1 \simeq 1.0$ mmHg, has several difficulties. Consider the feasibility of the quasi-steady-state of supersonic flow around a model under these conditions. The boundary layer on the shock tube wall acts as an aerodynamic sink through which the gas escapes from the hot region behind an incident SW. This accelerates the contact surface, decelerates the shock wave and, as a consequence, the distance between the contact surface and the SW front shortens. The time of existence of the steady-state gas dynamic conditions behind a SW, τ_{st}, taking into account the interaction between the flow and the laminar boundary layer on the ST wall is determined from the following relation [19]

$$2(\ln(1-\sqrt{\bar\tau_{st}})+\sqrt{\bar\tau_{st}})+\frac{\bar\tau_{st}}{W} = -X \qquad (2)$$

where $X = x_m/Wl_m$, x_m being the distance to the observation section,

$$\bar\tau_{st} = \tau_{st}/(l_m/u_s),$$
$$l_m = \frac{1}{W-1}\left(\frac{R_T}{2}\right)^2\left(\frac{\rho_2(u_s-u_2)}{\mu_2}\right)\beta^{-2}, \qquad (3)$$

$R_T = 3.8$ cm. At the Prandtl numbers $Pr = 0.67$, typical of the present work, the quantity β is determined from the relation [19]

$$\beta = 1.616\left(\frac{\rho_e\mu_e}{\rho_w\mu_w}\right)^{0.37}\left[1+\frac{1.043}{W-1}+O(W-1)^2\right]. \qquad (4)$$

The gasdynamic times τ_{st} obtained from equations (2)–(4) for the characteristic conditions of the present work are given in Fig. 1 for different velocities of the incident SW. This figure also contains the results of experimental determination of the value of τ_{st} from the measurements of the emission of O_2 molecules over the spectral interval of the Shuman–Runge band (the wave band is 4081 ± 2 Å). It is known that for the recombination-produced O_2 molecules the radiation intensity in this band is proportional to the square of the oxygen atom concentration [20]. Therefore, these measurements allow one to reliably determine the start of the hot gas region disintegration accompanied by a decrease in temperature and in the quasi-stationary concentration of [O] atoms and, consequently, by a sharp reduction in the strength of radiation. Measurements were made for oxygen–argon mixtures with the use of which, as is shown further, a substantial decrease in the velocity of incident shock waves can be attained which is essential for shock tube experiments. A good correlation between the measured and predicted τ_{st} values was observed. The values of τ_{st}

Table 1. The rate constants of chemical reactions (5)–(7) used in calculations [21]. The rate constants reactions are given in the form:

forward reactions $K_j = AT^a \exp\left(-\frac{E_a}{RT}\right)$ (cm^3 mol^{-1} s^{-1})

reverse reactions $K_{-j} = BT^b$ (cm^6 mol^{-2} s^{-1})

No. of reaction	A	a	E_a/P	B	b
5	2.3×10^{19}	-1	59400	1.9×10^{16}	$-1/2$
6	8.5×10^{19}	-1	59400	7.1×10^{16}	$-1/2$
7	3×10^{18}	-1	59400	2.5×10^{15}	$-1/2$

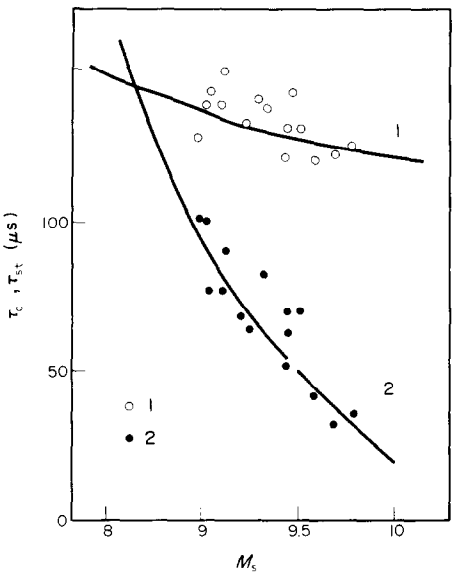

FIG. 1. The lifetime of the hot gas region τ_{st} (predicted curve 1 and experimental points 1) and time for the establishment of chemical equilibrium τ_c (curve 2 and points 2) as functions of the incident SW Mach number M_s. The mixture has initial composition of 20% O_2 + 80% Ar and P_1 = 1.0 mmHg.

somewhat decrease from the 150th to 120th μs on an increase of the SW Mach number from 8.5 to 10.

Behind the SW front there occurs the dissociation of O_2 molecules and the flow becomes a chemical nonequilibrium, and this also limits the duration of the steady-state flow past the model. The time of chemical relaxation behind the SW front, τ_c, was determined by numerically integrating the kinetic equations that describe the dissociation of O_2 molecules. Oxygen dissociation at high temperatures, $T \simeq 2000$–4000 K, is described by the following elementary stages [21]:

$$O_2 + O_2 \rightleftarrows O + O + O_2 \quad (5)$$

$$O_2 + O \rightleftarrows O + O + O \quad (6)$$

$$O_2 + M \rightleftarrows O + O + M \quad (7)$$

where M denotes the inert diluent molecule. The rate constants for the forward and reverse reactions (5)–(7) have been chosen according to ref. [22] and are given in Table 1.

The system of differential equations for the chemical kinetics of processes (5)–(7) was integrated numerically together with the relations that describe the mass, momentum and energy conservation laws in a one-dimensional isentropic flow behind the SW front in a coordinate system moving with the incident SW:

$$\rho u = \rho_1 u_1 \quad (8)$$

$$P + \rho u^2 = P_1 + \rho_1 u_1^2 \quad (9)$$

$$h + \frac{u^2}{2} = h_1 + \frac{u_1^2}{2}. \quad (10)$$

Subscript 1 in the above equations denotes the quantities describing the gas state ahead of the SW, while the unsubscripted quantities represent the instantaneous values of the compressed gas parameters behind the SW front. Integration was carried out with the use of the program [23] developed for rigid systems of differential equations which, in particular, include the equations of chemical kinetics. The relaxation time τ_c, used in the paper, corresponds to the time required by oxygen atoms to attain the values of concentration that differ from the equilibrium ones by less than 5%. The results of calculations and measurements of the chemical relaxation time τ_c are given in Fig. 1. The value of τ_c was also determined by recording emission of O_2 molecules in the Shuman–Runge band. It is seen that the time required to establish chemical equilibrium decreases sharply from $\tau_c \simeq 150$ μs at the incident SW Mach number $M_s \simeq 8.5$ to $\tau_c \simeq 20$ μs at $M_s \simeq 10$. This is associated with an increase in the compressed gas temperature and density which accelerates chemical conversion. A good agreement is observed between the measured and predicted results. At $M_s \gtrsim 8.5$, the time required for the establishment of chemical equilibrium, τ_c, becomes smaller than the gasdynamic time of existence of steady-state conditions in the hot gas region, τ_{st}, so that within the time interval $\Delta\tau_{exp} = \tau_{st} - \tau_c$ measurements in a gas flow with an equilibrium degree of dissociation are possible. It follows from Fig. 1 that at $M_s \gtrsim 9.5$ the time of quasi-steady-state equilibrium flow around a model comes to about 100 μs.

The results presented in Fig. 1 were obtained at an initial pressure of 1 mmHg in the shock tube. An increase of the initial pressure P_1 leads to an increase in the gasdynamic time τ_{st} and to a decrease of the time τ_c and, consequently, to an increase of the time $\Delta\tau_{exp}$.

At a characteristic initial gas pressure $P_1 = 1$ mmHg the boundary layer on the wall has a thickness commensurable with the shock tube diameter. The interaction between the gas flow and boundary layer alters the gas parameters along the hot gas region. The compressed gas pressure, temperature and velocity increase with the distance from the SW front attaining the steady-state values [24]. In the conditions considered this period superimposes on the time interval during which O_2 molecules dissociate behind the SW front. For this reason it is impossible to determine the time required for the establishment of the steady state. The control of the flow parameters on the completion of dissociation has shown that they change by no more than 2–3%. Consequently in the present conditions the time required for the flow parameters behind the SW to attain their steady-state values was smaller than that required for the dissociation of O_2 molecules.

Thus, a shock tube provides the possiblity for implementing a quasi-steady, supersonic flow of a dissociated gas around a model when the 'frozen' chemical composition of the gas in the boundary layer at the surface of the model is ensured. Since τ_{st} and τ_c for a multi-component gas can be calculated approximately and their values can be the same, it is

necessary that the parameters of a flow behind the SW be controlled in the experiments.

3. CALCULATION OF HEAT TRANSFER RATE TO A GAUGE

The steady-state gas parameters in the hot region for an equilibrium dissociated mixture were calculated numerically on the basis of the conservation equations (8)–(10) augmented with relations that describe chemical equilibrium in the system. Measurements of the heat transfer rate to the gauge were made on the surface of a plate near which the Prandtl–Meyer expansion of the supersonic flow takes place. The estimations of the Damkohler number for the gas parameters in the Prandtl–Meyer flow under the above ST operating parameters yield the values $\zeta_g \leqslant 2\times 10^{-5}$. The chemical composition of the gas in this case is frozen [1]. Under these conditions the Prandtl–Meyer function has the form [25]

$$\nu(M) = \sqrt{\frac{\kappa+1}{\kappa-1}}\arctan\sqrt{\frac{\kappa-1}{\kappa+1}(M^2-1)} - \arctan\sqrt{M^2-1} \quad (11)$$

where M is the Mach number in the Prandtl–Meyer flow. The final Mach number in the flow after expansion is determined as

$$\nu(M_e) = \nu(M_2)+\theta \quad (12)$$

where M_2 is the gas flow Mach number behind the SW associated with the measured quantity, i.e. the incident SW Mach number. The gas parameters in the Prandtl–Meyer flow and, consequently, those at the boundary-layer edge were calculated on the basis of the Mach number M_e which is determined, according to equations (11) and (12), by the relations given in ref. [25]. The heat transfer rate to the plate was determined by solving the system of equations for a frozen laminar boundary layer [26]

$$\frac{\partial \rho u}{\partial x}+\frac{\partial \rho v}{\partial y}=0 \quad (13)$$

$$\rho u\frac{\partial c_i}{\partial x}+\rho v\frac{\partial c_i}{\partial y}=\frac{\partial}{\partial y}(-J_i) \quad (14)$$

$$\rho u\frac{\partial u}{\partial x}+\rho v\frac{\partial u}{\partial y}=\frac{\partial}{\partial y}\left(\mu\frac{\partial u}{\partial y}\right) \quad (15)$$

$$\rho u\frac{\partial h_f}{\partial x}+\rho v\frac{\partial h_f}{\partial y}=\frac{\partial}{\partial y}\left(\frac{\mu}{Pr}\frac{\partial h_f}{\partial y}\right)+\mu\left(\frac{\partial u}{\partial y}\right)^2 + \frac{\partial}{\partial y}\left(\frac{\mu}{Pr}\sum_i\frac{C_p}{\lambda}J_i+\frac{\partial c_i}{\partial y}h_{fi}\right) \quad (16)$$

where $c_p=\sum_i c_i C_{pi}$ is the heat capacity of the mixture.

Under the experimental conditions typical of the present work the Reynolds number on the outer edge of the boundary layer varies within the range $Re = 5\times 10^3$–10^4. In these conditions the outer flow interacts weakly with the boundary layer, the interaction parameter does not exceed 0.2, i.e. it can be assumed to a good approximation that $dP_e/dx = 0$ [27]. The boundary conditions in this approximation are

$$\begin{aligned} &\text{at } y=0 \quad u=v=0, \quad h_f=h_{fw}, \quad J_3=0\\ &y=\infty \quad u=u_e, \quad v=0, \quad h_f=h_{fe}, \quad c_i=c_{ie}\\ &x=0 \quad u=u_e, \quad v=0, \quad h_f=h_{fe}, \quad c=c_{ie} \end{aligned} \quad (17)$$

where the subscript w refers to gas parameters at the plate surface. Assuming that atom recombination on the surface follows the first order and the shock mechanism, the following boundary condition will hold at $y = 0$

$$-J_1 = J_2 = K_w\rho_w c_{1w},$$

where the heterogeneous recombination rate constant is determined as

$$K_w=\gamma_w\sqrt{\frac{RT_w}{2\pi m_1}}. \quad (18)$$

The heat flux to the surface is determined by the relation [1]

$$Q_{wt}=\left(\frac{\mu}{Pr}\frac{\partial h_f}{\partial y}\right)_w+(J_1 h_1^0)_w \quad (19)$$

where the first term is the conduction heat flux Q_c and the second term is the recombination heat flux Q_r.

The diffusion fluxes are determined from the Stefan–Maxwell relations [27]. For the ternary mixtures being considered, i.e. O, O_2 and Ar, in which the inert solvent (argon) is much in excess of the molecular and atomic oxygen $c_3 \gg c_1, c_2$, these relations can be simplified considerably. It can be assumed for these conditions that $J_3 = 0$ and $c_3 = c_{3e} = \text{const.}$ which satisfy the diffusion equation (14) with boundary conditions (17). With this taken into account, it follows from the Stefan–Maxwell relations that the diffusional fluxes of molecular and atomic oxygen are of the same magnitude but of opposite direction

$$-J_2 = J_1 = -\rho D_{13}\frac{\partial c_1}{\partial y}\delta \quad (20)$$

where D_{13} is the binary diffusion coefficient of the oxygen atoms in argon and δ is the correction term accounting for the multi-component nature of diffusion. In the present work, for the mixture O–O_2–Ar, the following was obtained:

$$\delta^{-1}=\frac{D_{13}}{D_{12}}(1+c_1)\left(c_2\frac{m}{m_2}+c_1\frac{m}{m_2}\right)+c_3\frac{m_3}{m} \times\left(1+c_1\frac{m_3-m_1}{m_1}\right)+\frac{D_{13}}{D_{23}}c_1c_3\frac{m(m_3-m_2)}{m_2m_3} \quad (21)$$

where D_{ik} are the corresponding diffusion coefficients and m is the molecular weight of the mixture.

The calculations have shown that with a change in

the mixture composition within $T = 300$–4000 K from the binary one, $O_2 + Ar$, at low temperatures up to that corresponding to virtually complete oxygen dissociation at high gas temperatures, the value of δ lies within the range 0.97–1.02, i.e. it stays practically constant. Therefore, for the diffusion of oxygen atoms it is possible to assume that $\delta = 1$. Then relation (20) reduces to the Fick law with the effective diffusion coefficient coinciding with the coefficient of binary diffusion in the mixture O–Ar–D_{13}.

In the conditions considered the energy conservation equation (16) can also be simplified. The last term in this equation, with allowance for equation (20) and the assumption that $J_3 = 0$ and $c_3 = \text{const.}$, is

$$\frac{\partial}{\partial y}\left[\frac{\mu}{Pr}(Le-1)\left(h_{1f}\frac{\partial c_1}{\partial y}+h_{2f}\frac{\partial c_2}{\partial y}\right)\right]. \tag{22}$$

Since for the specific enthalpies of the molecular and atomic oxygen $h_{1f} \simeq h_{2f}$ also in the case considered, i.e. at $c_3 \gg c_1, c_2$, $\partial c_1/\partial y = -\partial c_2/\partial y$, and since, as will be shown later, the Lewis–Semyonov number varies within the range $Le = 1.2$, the estimations show that the term (22) does not exceed 1% of the value of the first term of the RHS of equation (16), i.e. $\partial/\partial y[(\mu/Pr)(\partial h/\partial y)]$. Therefore the term (22) in the energy conservation equation (16) was neglected in this work.

The calculation of the transport coefficients: binary diffusion D_{ik}, viscosity μ and thermal conductivity λ, for the conditions of this work is given in the Appendix. These were used to determine the Prandtl number $Pr = (\mu c_p)/\lambda$, the Lewis–Semyonov number $Le = (\rho D_{13} c_p)/\lambda$ and the Schmidt number $Sc = \mu/\rho D_{13}$ required for calculations. Figure 2 presents the results of calculations of the numbers Pr, Le and Sc in the range of temperatures at the outer edge of the boundary layer typical of this work, i.e. $T_e = 2500$–5000 K. It is seen that a change in these numbers does not exceed 5%. For the conditions in the gas near a cold wall ($T_w = 300$ K) these numbers constitute: $Pr_w = 0.67$, $Sc_w = 0.53$ and $Le_w = 1.26$ for an ideally catalytic surface ($\gamma_w = 1$), and $Pr_w = 0.56$, $Sc_w = 0.58$, $Le_w = 0.96$ for a non-catalytic surface ($\gamma_w = 0$). The numbers Pr, Le and Sc on a cold wall differ from those on the boundary-layer outer edge by not more than 10%. Therefore their change across the boundary layer was not taken into account in this work. For the conditions on the boundary-layer edge and near the surface, mean values of Pr, Sc and Le numbers were used in calculations.

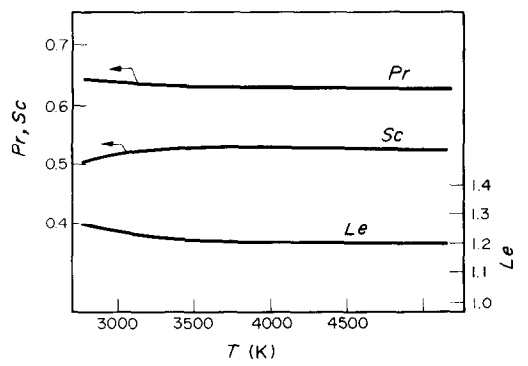

FIG. 2. The Prandtl, Schmidt and Lewis–Semyonov numbers (Pr, Sc, Le) at the outer boundary-layer edge vs the gas temperature. The initial conditions and mixture composition are same as for Fig. 1.

In the Dorodnitsyn–Lees variables, η and ξ, which for the flat plate case [1] have the form

$$\eta = \frac{\rho_e u_e}{\sqrt{2\xi}}\int_0^y \frac{\rho}{\rho_e}\,dy; \quad \xi = \rho_e u_e \mu_e x, \tag{23}$$

the simplified, for the conditions considered, system of boundary-layer equations is written as

$$\frac{\partial}{\partial\eta}\left(l\frac{\partial\omega}{\partial\eta}\right)+f\frac{\partial\omega}{\partial\eta} = 2\xi\left(\omega\frac{\partial\omega}{\partial\xi}-\frac{\partial f}{\partial\xi}\frac{\partial\omega}{\partial\eta}\right) \tag{24}$$

$$\frac{\partial}{\partial\eta}\left(\frac{l}{Pr}\frac{\partial g}{\partial\eta}\right)+f\frac{\partial g}{\partial\eta}+\frac{u_e^2}{h_{fe}}l\left(\frac{\partial\omega}{\partial\eta}\right)^2 = 2\xi\left(\omega\frac{\partial g}{\partial\xi}-\frac{\partial f}{\partial\xi}\frac{\partial g}{\partial\eta}\right) \tag{25}$$

$$\frac{\partial}{\partial\eta}\left(\frac{l}{Sc}\frac{\partial z}{\partial\eta}\right)+f\frac{\partial z}{\partial\eta} = 2\xi\left(\omega\frac{\partial z}{\partial\xi}-\frac{\partial f}{\partial\xi}\frac{\partial z}{\partial\eta}\right). \tag{26}$$

In terms of the new variables, boundary conditions (17) are:

on the plate surface

$$\text{at } \eta = 0 \quad f = w = 0, \quad g = \frac{h_{fw}}{h_{fe}}, \quad \frac{\partial z}{\partial\eta} = \zeta_w z$$

on the boundary-layer outer edge

$$\begin{aligned} &\text{at } \eta = 0 \quad w = g = z = 1 \\ &\text{at } \xi = 0 \quad w = g = z = 1 \end{aligned} \tag{27}$$

where $\rho_w = \tau_d/\tau_r = (Sc_w/l_w)(\rho_w K_w/\rho_e u_e)\sqrt{2Re_x}$ is the surface recombination reaction Damkohler number on a streamlined flat plate surface, being the ratio of the time for the diffusion of atoms through the boundary layer to the characteristic time of heterogeneous recombination on the surface.

The estimations show that a change in the quantity l along the boundary layer does not exceed 10%, while across the boundary layer, in the direction toward the surface, this quantity may increase several times. These changes of the quantity l have a weak effect on the results of calculations of heat fluxes. For example, the assumption that $l = \text{const.}$ allows one to carry out calculations accurate to within 3–5% [1]. Since the results obtained depend weakly on l, only its transverse variation was allowed for in the present work, i.e. it was assumed that $l(\eta, \xi) = l(\eta)$. Equation of motion (24) and boundary condition (27) in the approximation made are invariant against the change in the scale in terms of the variable ξ and are therefore self-similar.

Since due to the self-similarity of equation (24) $\partial f/\partial\xi = 0$, the RHS of equation (25) has the form

$$2\xi\omega\frac{\partial g}{\partial\xi}.$$

Based on equation (20) and the condition that $c_3 = \text{const.}$, the RHS of equation (25) can be rewritten in the form

$$2\xi\omega\frac{\partial z}{\partial\xi}\left(1-\frac{h_{f_2}}{h_{f_1}}\right)c_{1e}\frac{h_{f_1}}{h_{f_e}}. \tag{28}$$

This term can be neglected near the surface, since $\omega \to 0$. At a distance from the surface, this term can be neglected as compared, for example, with the second term of the LHS of equation (25), $f(\partial g/\partial\eta)$, since $f \gtrsim \omega \sim 1$ [1], in the conditions of the present work $[1-(h_{f_2}/h_{f_1})c_{1e}(h_{f_1}/h_{f_e})] \lesssim 0.03$, and as was found by calculations, $\partial g/\partial\eta \gtrsim 2\xi(\partial z/\partial\xi)$.

In the assumptions made the system of equations (24)–(26) can be written as

$$\frac{\mathrm{d}}{\mathrm{d}\eta}\left(l\frac{\mathrm{d}\omega}{\mathrm{d}\eta}\right)+f\frac{\mathrm{d}\omega}{\mathrm{d}\eta}=0 \tag{29}$$

$$\frac{\mathrm{d}}{\mathrm{d}\eta}\left(\frac{l}{Pr}\frac{\mathrm{d}g}{\mathrm{d}\eta}\right)+f\frac{\mathrm{d}g}{\mathrm{d}\eta}+\frac{u_e^2}{h_{fe}}l\left(\frac{\mathrm{d}\omega}{\mathrm{d}\eta}\right)^2=0 \tag{30}$$

$$\frac{\partial}{\partial\eta}\left(\frac{l}{Sc}\frac{\partial z}{\partial\eta}\right)+f\frac{\partial z}{\partial\eta}=2\xi\omega\frac{\partial z}{\partial\xi}. \tag{31}$$

In terms of the variables η and ξ the relation for the heat flux to the surface (19) acquires the form

$$Q_{wt}=\frac{l_w}{Pr}\frac{\rho_e u_e}{\sqrt{2Re_x}}\left[h_{fe}\frac{\partial g}{\partial\eta}(0)+Leh_1^0c_{1e}\frac{\partial z}{\partial\eta}(0,\xi)\right] \tag{32}$$

where, similar to equation (19), the first and the second terms in square brackets describe the conduction and recombination heat fluxes, respectively. Thus, so that the heat flux Q_{wt} could be recovered, it is necessary to determine the quantities $\partial g/\partial\eta(0)$ and $\partial z/\partial\eta(0,\xi)$, solving the system of equations (29)–(31).

The solution of system (29)–(31) with boundary conditions (27) was made numerically by the method of straight lines. The partial differential equation (31) was replaced by the differential-difference relation

$$\frac{\mathrm{d}}{\mathrm{d}\eta}\left(\frac{l}{Sc}\frac{\mathrm{d}z_n}{\mathrm{d}\eta}\right)+f\frac{\mathrm{d}z_n}{\mathrm{d}\eta}=2\omega\xi_n\frac{z_n-z_{n-1}}{\Delta\xi} \tag{33}$$

where $z_n(\eta)$ is the dimensionless concentration of oxygen atoms on the nth straight line $\xi_n = \text{const.}$ Relation (33), which is an ordinary differential equation, allows one to successively determine the function $z_n(\eta)$ on the $\xi_n = \text{const.}$ straight line on the basis of the known function $z_{n-1}(\eta)$ on the preceding straight line $\xi_{n-1} = \text{const.}$

The derivative with respect to ξ in relation (33) was approximated to the first order of accuracy to impart additional stability for calculations of the gas parameters in the boundary layer near the surface was discontinuous catalytic properties [28]. It was found that in the case of discontinuous catalytic properties the convergence is achieved when $\Delta\xi \lesssim 0.01$. The method is an implicit one and as a result no difficulties arise which are usually associated with the instability of numerical calculation.

The system of ordinary differential equations (29)–(31) was integrated numerically. In order to satisfy boundary conditions (27), the ranging method was employed. The values of $\mathrm{d}\omega/\mathrm{d}\eta$, $\mathrm{d}g/\mathrm{d}\eta$ and z at $\eta = 0$ were determined which would ensure, as a result of solving the system of equations, the coincidence of the obtained values of the functions ω, h and z at the outer boundary-layer edge with boundary conditions (31) for $\eta = \infty$. In this case the values of $\mathrm{d}\omega/\mathrm{d}\eta$, $\mathrm{d}g/\mathrm{d}\eta$ and of z at $\eta = 0$ were recovered by the Newton method with an error not exceeding 0.1%.

In order to check the developed method of calculation for the conditions of works [29–31], the dimensionless concentration of oxygen atoms on the surface z_w was calculated for a flat plate with constant catalytic properties. Just as in refs. [29–31], it was assumed that $l = \text{const.}$ across the boundary layer. The values of z_w, that were determined earlier in refs. [29–31] and in this work (in the assumptions according to refs. [29–31], curve 1), are given in Fig. 3 as functions of the Damkohler number ζ_w. One can see a good, within 1%, coincidence between the results of the present calculations and those [29] made by the series expansion method and numerical integration; by the solution with the use of asymptotic relations for a boundary layer [30]; and with the use of the integral method [31]. Calculations for the conditions of works [29–31] with regard for a change in the quantity l across the boundary layer shows that the dimensionless concentration z_w may differ by 2–3% and this is essential for the heat flux recovery. Therefore, the transverse variation of the quantity l should be taken into account. Thus, as compared with earlier techniques [29–31], the method developed is more simple and at the same time it ensures a higher accuracy of calculation.

When recovering the probabilities of heterogeneous recombination [15, 17] to calculate the heat transfer rate to the flat plate surface, an analytical method of

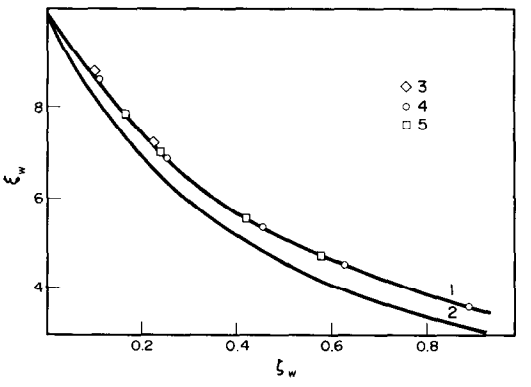

FIG. 3. Dimensionless surface concentration of oxygen atoms z_w as a function of the Damkohler number ζ_w for flat plate with constant catalytic properties ($\gamma_w = \text{const.}$). Curve 1 presents the results of calculations by the technique of the present work; 2, by the local similarity method [17]; 3, the results of ref. [29]; 4, of ref. [30]; 5, of ref. [31].

local similarity [17] was used. The concentration z_w calculated in the present work with the use of the local similarity method [15, 17] are given in Fig. 3 by curve 2. It is seen that the local similarity method understates the atomic oxygen concentration near the surface by 5–10%. By virtue of relation (32), approximately the same understating is observed for the recombination heat flux. According to study [1], this may lead to the overstation of the experimentally measured value of γ_w (the catalytic activity coefficient) by more than an order of magnitude.

The local similarity method [17] leads to still greater errors when the plate surface has a discontinuous catalytic activity, e.g. when only a portion of the plate is covered with the substance studied. This can be attributed to the disregard of the plate longitudinal coordinate derivatives in the conservation equations [17]. Figure 4 contains the results of calculation, by the method developed in the present work, of the total heat flux Q_{wt} to the plate surface having a discontinuity catalycity $\gamma_w = 0$ at $0 \leqslant x \leqslant 1.0$ cm and $\gamma_w = 0.05$ at $x \geqslant 1.0$ cm for the conditions pertaining in these experiments on shock tubes (curve 1). Curve 2 presents the results of calculation by the local similarity method [17].

It is seen that the heat flux at the leading edge of the catalytic material ($x = 1.0$ cm) has high values, about 100 cal cm^{-2} s^{-1}, decreasing with distance down to about 60 cal cm^{-2} s^{-1} at $x \simeq 1.4$ cm; a decrease in the heat flux during gas motion over the catalytic surface is associated with a decrease in the amount of atoms in the wall layer as a result of their recombination on the face. The calculation of the heat flux by the local similarity method [17] for large distances from the leading edge of catalytic material, $x \gtrsim 1.4$ cm, understates the heat transfer rate by 5–10%, qualitatively corresponding to the data given in Fig. 3 for a plate with constant catalytic properties. Near the leading edge of the catalytic material the value of Q_{wt}, calculated according to ref. [17], is underestimated by more than a factor of two.

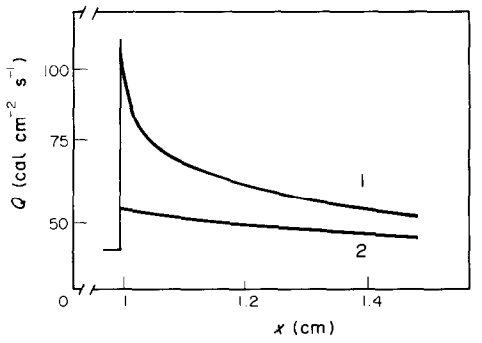

FIG. 4. Total heat flux Q_{wt} to a plate with discontinuous catalytic properties: $\gamma_w = 0$ at $x < 1.0$ cm and $\gamma_w = 0.05$ at $x \geqslant 1$ cm. Curve 1, the results obtained by the technique suggested in the present work; 2, from ref. [17] in the conditions typical of the shock tube experiments: initial pressure $P_1 = 1$ mmHg; initial composition of mixture 20% O_2 + 80% Ar; SW velocity $u_s = 3.0 \times 10^5$ cm s^{-1}; Reynolds numbers for the gauge are $Re_x = 2.8 \times 10^3$ which correspond to the following gas parameters at the boundary-layer edge: $u_e = 2.8 \times 10^5$ cm s^{-1}, $P_e = 90$ mmHg, $T_e = 3245$ K and mixture composition of 30% O + 2% O_2 + 68% Ar.

4. OPTIMIZATION OF MIXTURE COMPOSITION

The fraction of heat flux to the model in a supersonic gas flow due to atom heterogeneous recombination Q_r for the case of supersonic flow past a model does not exceed several tens percent of the total heat flux Q_{wt} to the surface. The recombination portion of the heat flux to the flat plate in a supersonic flow is proportional to the ratio between the enthalpy of dissociation oxygen molecule h_D and the total enthalpy of the mixture $h_t = h_D + C_pT + u^2/2$ [17]. Therefore, the optimum conditions are achieved when the mixture is heated to the temperatures of practically complete dissociation of molecular oxygen. This is illustrated by calculations of the ratio between the recombination and total enthalpies, h_D/h_t, given in Fig. 5 as a function of the incident shock wave Mach number M_s. Calculations were made for mixtures of the initial composition O_2–Ar with the molecular oxygen content varying from 20 to 100% within the range of the incident wave Mach numbers $M_s = 8$–20. The total enthalpy was calculated for the equilibrium state of the gas, dissociated behind the shock wave, being determined from conservation equations (8)–(10). The curves corresponding to each of the mixtures investigated have their maxima at certain values of $M_s = M_{s,max}$. When $M_s > M_{s,max}$, the molecular oxygen is almost completely dissociated and

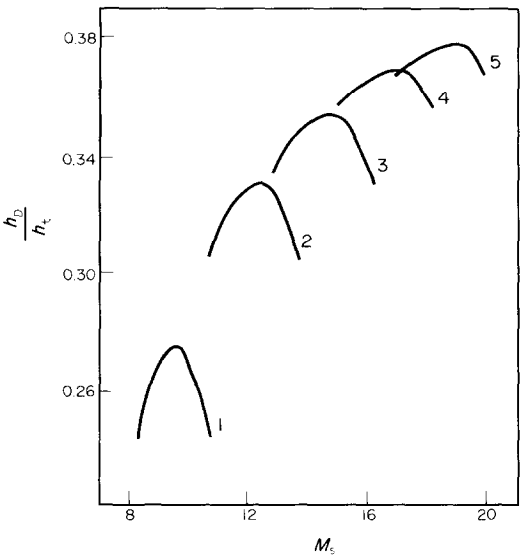

FIG. 5. The ratio of the oxygen dissociation enthalpy h_D to the total gas enthalpy h_t as a function of the incident SW Mach number M_s for O–Ar mixtures containing different amounts of molecular oxygen. Curve 1 corresponds to the mixture with the initial composition of 20% O_2 + 80% Ar; 2, 40% O_2 + 60% Ar; 3, 60% O_2 + 40% Ar; 4, 80% O_2 + 20% Ar; 5, pure O_2; $P_1 = 1$ mmHg.

there is no further increase of the enthalpy h_D, while the value of h_t increases as a result of increase of the gas temperature and of the kinetic energy of the flow, which leads to a decrease of the ratio h_D/h_t.

The calculations show that the optimum incident SW Mach numbers decrease substantially from $M_s \simeq 20$ to $M_s \simeq 9$ with a decrease of the oxygen content in the mixture with an inert diluent (argon) from 100% (curve, 5, Fig. 5) to 20% (curve 1, Fig. 5). The fraction of the dissociation enthalpy h_D in the total enthalpy h_t for these mixtures at respective optimum SW Mach numbers decreases insignificantly from 38 to 28%. The use of mixtures that contain about 20% oxygen allows one to significantly reduce the intensity of incident SWs with an insignificant decrease in the magnitude of the recombination heat flux Q_r and, consequently, in the accuracy of the recovery of heterogeneous recombination probability γ_w. The possibility for the reduction of the shock wave intensity by a suitable choice of mixture composition simplifies experimental procedures on shock tubes.

5. GAUGE GEOMETRY OPTIMIZATION

The catalytic activity of investigated materials in a supersonic flow of gas dissociated behind a SW was determined by a gauge in the form of a narrow plate with a sharp leading edge placed at a small expansion angle to the flow [17]. This geometry allows rather an accurate determination of the state of the gas interacting with the surface thus reducing the error in the recovery of the heterogeneous recombination probability γ_w on the basis of the measured heat flux.

A flat wedge-like plate has some advantages over wide-spread blunt bodies on which measurements of the heat transfer rate in the vicinity of the stagnation point are carried out. In front of the blunt-body-type models a strong shock wave is formed which may cause additional dissociation of gas near the surface which is ignored in calculations of heat fluxes. Sometimes the gas dynamics of flow becomes very complex and this makes it necessary to take into account the second-order effects, i.e. free stream vorticity, its displacement by the boundary layer, slippage and temperature jump on the surface [32]. These factors increase the uncertainty of calculations of heat fluxes and, consequently, the error in the recovery of the heterogeneous recombination probability γ_w.

Another heat flux gauge was also suggested [15], the sentitive element of which was a heat resistor made of a plate 0.1-μm thick in the form of a band, about 1-mm wide, placed at a distance of several millimeters from the plate leading edge. The substance studied was applied to the surface of an insulating layer of silicon monoxide over the entire surface of the plate or its greater portion. This geometry of the heat flux gauge is not an optimum one from the viewpoint of ensuring the maximum relative magnitude of the recombination heat flux Q_r especially when investigating the substances with high catalytic activity; in fact when the gas moves along the plate, there occurs, due to heterogeneous recombination, a decrease in the monatomic oxygen concentration z_w near the surface. Therefore, at the location of the heat resistor the recombination heat flux Q_r, which in particular is proportional to z_w, also decreases. To ensure the maximum value of the recombination heat flux it is suggested in the present work that the substance investigated be applied only over a narrow band of a heat resistor at a distance from the leading edge and that the space between the substance and the plate leading edge be covered with substances having a minimal catalytic activity.

Figure 6 presents the ratios of the difference of total heat fluxes to catalytic and non-catalytic surfaces, $\Delta Q_{wt} = Q_{wt}(\gamma_w) - Q_{wt}(\gamma_w = 0)$ to the quantity $Q_{wt}(\gamma_w)$, which were calculated in the present work for different surface recombination Damkohler numbers ζ_w. This ratio of heat fluxes determines the sensitivity of the method considered. The calculations were carried out for the conditions pertaining to the experiments on shock tubes following the technique described in Section 3. The prescribed incident shock wave velocity gave the equilibrium gas parameters after the completion of the dissociation of O_2 molecules. Based on the determination of the state of the gas, having expanded into a Prandtl–Meyer flow near the plate, the parameters on the boundary-layer edge were recovered and then the boundary-layer equations were solved to determine heat fluxes.

Curve 1 in Fig. 6 presents calculations for the

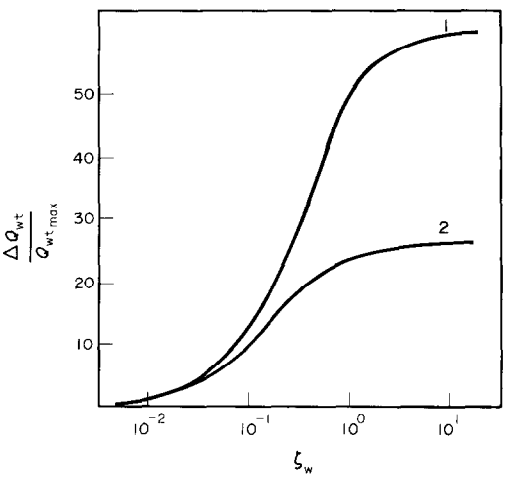

FIG. 6. The dependence of the quantity $\Delta Q_{wt}/Q_{wt}(\gamma_w)$ on the surface Damkohler number ζ_w in the conditions typical of ST experiments: expansion angle of the plate $\theta = 5°$; initial gas pressure $P_1 = 1$ mmHg; initial composition of mixture 20% O_2 + 80% Ar; velocity of the incident SW $u_s = 3.0 \times 10^5$ cm s^{-1} ($M_s = 9.5$); the gauge Reynolds numbers $Re_x = 2.8 \times 10^3$ which correspond to an equilibrium composition of the free stream, 30% O + 2% O_2 + 68% Ar, and to gas parameters on the boundary-layer edge: flow velocity $u_e = 2.8 \times 10^5$ cm s^{-1}, pressure $P_e = 90$ mmHg, temperature $T_e = 3245$ K. Curve 1 presents the results of calculations for the gauge of refs. [15, 17]; 2, for the gauge suggested in the present work.

geometry of the gauge [15, 17] whose entire surface, from the leading edge of the plate to the sensitive element, $0 \lesssim x \lesssim 1.0$ cm, is covered with the substance studied; curve 2, for the gauge suggested in the present work in which the material investigated covers only the sensitive element, i.e. the heat resistor $\Delta x = 0.1$-cm wide located at a distance of $x = 1$ cm from the leading edge, while the surface between the leading edge and the heat resistor is non-catalytic, $\gamma_w = 0$.

It follows from Fig. 6 that with the characteristic accuracy of heat flux measurements of 2–5% [33] the catalytic recombination coefficient can be recovered for the gauge developed in the present work in the range of Damkohler numbers $0.02 \lesssim \zeta_w \lesssim 10$ and for the gauge suggested in works [15, 17] in the range $0.02 \lesssim \zeta_w \lesssim 1.0$. When $\zeta_w \lesssim 0.02$, the recombination heat flux does not exceed 1–2% of $Q_{wt} \approx Q_c$ and cannot be recorded reliably. When $\zeta_w \gtrsim 1$–10, the fraction of the recombination heat flux Q_r is appreciable and it amounts (depending on the type of the probe) to 50–60% of the total heat flux to an ideally catalytic surface Q_{wt} ($\gamma_w = 1$). However, in this case the value of Q_r does not depend on the heterogeneous recombination probability γ_w since practically all of the atoms near the surface recombine.

The calculations show that for the proposed geometry of the probe the fraction of the recombination heat flux Q_r increases appreciably (curve 2) as compared with the probe suggested in works [15, 17] (curve 1), especially in the region of the Damkohler numbers $\zeta_w \geqslant 0.5$. This noticeably extends the sentivity region of this catalytic recombination coefficient recovery method and increases its accuracy. For the conditions typical of the experiments on shock tubes ($M_s = 9.5$; $P_1 = 1$ mmHg; angle of plate slope $\theta = 5°$, the sensitive element is at a distance of $x = 1.0$ cm from the leading edge) this range of sensitivity with respect to the Damkohler number $0.02 \lesssim \zeta_w \lesssim 10$ corresponds to a change in the heterogeneous recombination probability $1 \times 10^{-3} \lesssim \gamma_w \lesssim 0.5$. This range comprises low-catalytic silicon-type materials for which $\gamma_w = 10^{-5}$–10^{-3}, metal oxides with $\gamma_w = 10^{-3}$–10^{-1}, a number of metals with $\gamma_w \lesssim 0.2$–0.3 and other materials.

To extend the region of sensitivity to the side of low values of γ_w, $\gamma_w \lesssim 1.0 \times 10^{-3}$, when the recombination heat flux Q_r is negligible, it is necessary that the gauge geometry and the supersonic flow parameters be changed so that the Damkohler numbers for the heterogeneous recombination of atoms ζ_w could be increased. According to equation (27), this can be achieved by increasing the distance from the heat resistor to the plate leading edge and also the plate expansion angle (with the provision of a non-separation flow mode). The extension of the sensitivity region for high values of ζ_w ($\zeta_w \gtrsim 0.5$) requires the lowering of the Damkohler number ζ_w which can be achieved by a reverse change of the above parameters. Thus, the method developed provides the overlap of practically the entire region of the catalytic recombination probabilities of the materials studied.

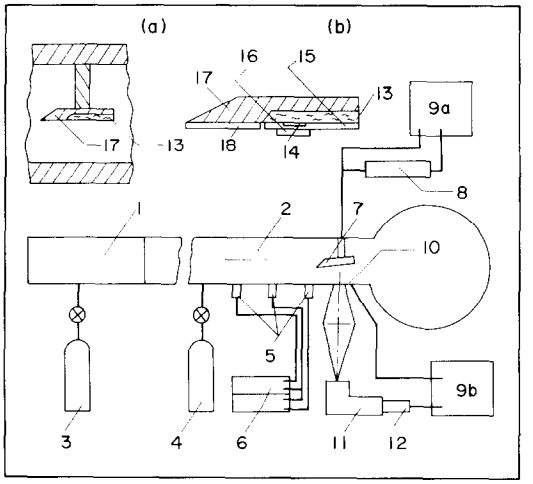

FIG. 7. Schematic diagram of an experimental setup: 1, driver section of a ST; 2, low-pressure (driven) section of a ST; 3, balloon with a driving gas; 4, balloon with a mixture of gases investigated; 5, piezoelectric pressure transducer; 6, frequency meters; 7, holder with a thin-film heat flux gauge; 8, analog scheme which recovers the heat flux value; 9(a,b), oscillographs; 10, wall resistors; 11, monochromator; 12, photomultiplier; 13, quartz plate with deposited thin-film platinum heat resistor; 14, 15, insulating film of oxidized SiO; 16, film of the substance studied; 17, heat flux gauge holder; 18, quartz film (SiO_2).

6. EXPERIMENTAL SETUP

Investigations were carried out on a 76-mm-i.d. shock tube made of stainless steel with the lengths of the driver section (1) of 1.5 mm and low-pressure (driven) section (2) of 5.5 m (Fig. 7). The low-pressure section was evacuated to have the residual pressure less than 10^{-2} mmHg. The shock tube was driven with hydrogen (3). In accordance with the calculations made in Section 5, the working mixture was used with the initial composition of 20% O_2 + 80% Ar (4). Before and after the measurements of the value of γ_w, calibration of the heat flux gauge was achieved during its blowing by pure argon heated in an incident shock wave. The initial pressure of P_1 of the gas investigated was in the range 0.7–2.0 mmHg, the incident SW Mach number was 5–8 during calibration and 9–11 during measurements making it possible to obtain approximately the same values of the heat flux. The shock wave velocity was recorded on two bases with the aid of three piezoelectric transducers (5) and two frequency counters (6). The heat flux gauge (7) was positioned at the end of the low-pressure section on a special holder having low aerodynamic resistance and occupying less than 7% of the shock tube cross section. This introduced only slight disturbance into the supersonic flow behind the incident shock wave. The signal from the heat flux gauge sensitive element was fed-in directly at an oscillograph (9a) and analogue scheme (8) [33] allowing one to recover the heat flux Q_{wt} by a change in the surface temperature. The heat flux to the gauge

surface was displayed by the second ray of the oscillograph (9a). Measurement of the surface temperature T_w at the characteristic time of plate blowing of about 100 μs did not exceed 1–3 K.

In this cross-section of the shock tube, measurements were simultaneously made of the side surface temperature by a wall platinum resistor (10) and the control of the content of atomic oxygen in the heated mixture by the intensity of O_2 emission in the Shuman–Runge band $B^3\Sigma_u^- - X^3\Sigma_g^+$, at the wavelength $\lambda = 4081 \pm 2$ Å which corresponds to a most intensive vibrational transition, relations (1) and (19). The required spectral interval was selected by a monochromator (11) and the emission was recorded by a photomultiplier (12). The photomultiplier signal and the signal from the wall heat resistor (10) were recorded by an oscillograph (9b).

The design of the heat flux gauge (7) is shown in boxes 'a' and 'b' of Fig. 7. The gauge is a quartz plate (13) measuring 22 × 20 × 3 mm with two welded platinum wires between which a heat resistor, which is a platinum film 2-mm wide and 0.1-μm thick (14), was applied by the fire-fitting technique. The distance from the platinum film to the leading edge of the holder was 18 mm. The gauge surface (13) was covered, by the method of vacuum deposition, with a thin layer of silicon monoxide, SiO, about 0.1-μm thick (15) which was then oxidized in air. Over this SiO film, above the heat resistor the studied substance to be studied was applied by the method of vacuum deposition or by the fire-fitting technique, 0.1-μm thick (16). In order to prevent damage to the quartz plate by supersonic flow the plate was placed into a metallic holder (17) with a sharp leading edge. The front side of the holder was covered with a SiO_2 film of thickness 0.5–1.0 μm (18) by the method of vacuum deposition. The holder surface (17) and the working surface of the quartz plate (13) were placed at the expansion angle 5° to the supersonic flow. It was found experimentally that the time resolution of the heat flux gauge did not exceed 5 μs.

A typical oscillograph trace of the experimental measurements of the catalytic recombination coefficient obtained for a mixture of the initial composition of 20% O_2 + 80% Ar is given in Fig. 8(a), an oscillogram of the calibrating experiment with a pure argon is given in Fig. 8(b). In the 20% O_2 + 80% Ar mixture, after the incident shock wave has passed the gauge (the time instant A), the equilibrium degree of disssociation is being established during the time interval $A - B$ as well as the approach of the supersonic flow parameters to the steady-state values, which can be clearly seen on the traces of the recombinational luminescence of oxygen (curve 1, Fig. 4(a)). The characteristic duration of the period of establishment was 50–120 μs for the conditions of the present work.

This if followed by the time period ($B - C$) 100–200 μs during which the supersonic flow parameters remain practically constant (1, Fig. 8(a)). In this case, the gauge surface temperature increases with time almost as $\sqrt{t}$ (3, Fig. 8(a)), while the heat flux to the surface is constant (2, Fig. 8(a)). During this time, measurements of the quasi-steady-state heat flux Q_{wt} were made whose comparison with the predicted values gave the heterogeneous recombination probability, γ_w, for oxygen atoms on the surface of the material investigated. Starting from the time instant, denoted by arrow 'c' in Fig. 8(a), cold gas arrives to the gauge from the region of the contact surface. In calibrating experiments with pure argon (Fig. 8(b)) the initial period of establishment, $A - B$, is a short one, about 20–

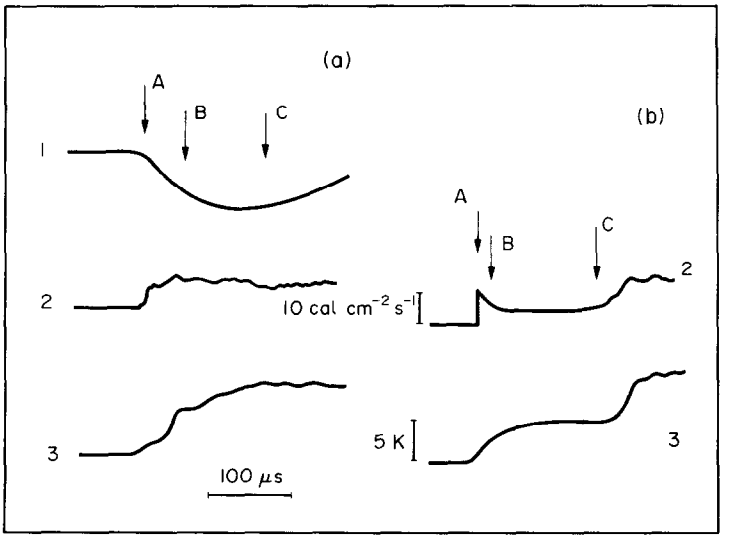

FIG. 8. Typical oscillograms: (a) working mixture with initial composition of 80% Ar + 20% O_2, $P_1 = 0.96$ mmHg, the equilibrium temperature and gas pressure behind the incident SW: $T_2 = 3500$ K, $P_2 = 105$ mmHg; (b) calibration experiment with a pure argon at $P_1 = 1.19$ mmHg, $T_2 = 3840$ K, $P_2 = 57$ mmHg. Curve 1, recombination emission of oxygen in the Shuman–Runge band; 2, total heat flux Q_{wt} to the surface; 3, temperature T_w of the film heat resistor.

40 μs, which is followed by a long period $B-C$, of the quasi-steady-state flow past a model lasting 100–250 μs.

7. RESULTS OF MEASUREMENTS OF THE PROBABILITY OF HETEROGENEOUS RECOMBINATION OF OXYGEN ATOMS ON SILICON OXIDE, ALUMINA AND PLATINUM

The results of some of the experiments are presented in Table 2. The gauge surface temperature T_w amounted to about 300 K. A platinum film was applied to a quartz substance by fire-fitting a platinizing paste solution following the procedure suggested in ref. [35]. Aluminum and silicon monoxide were applied by vacuum deposition. Gauges with platinum and silicon monoxide films were kept in air at room temperature for a week. Aluminum gauges were subjected to long heating up to 600 K in the oxygen atmosphere to form a stable oxidic film. No additional cleaning of the surface of the gauges was made after their oxidizing.

Table 3 summarizes the available results on the probability of heterogeneous surface recombination of oxygen atoms at $T_w = 300$–400 K obtained by different methods. It is known that the results may depend strongly on the state of the surface, gas pressure and a number of other experimental conditions. Therefore Table 3 also contains brief appropriate information.

8. DISCUSSION OF RESULTS

The methods of investigation of the recombination activity of materials can be subdivided into two large groups. The first, more numerous, is characterized by the determination of γ_w for a quiescent or slowly moving (several m s^{-1}) dissociating low-density gas interacting with the surfaces investigated. These are: the method of side sleeve, different types of continuous-flow reactors and reactive vessels [4–7, 36–41]. The second group covers the methods of heterogeneous recombination probability recovery by measuring heat fluxes to models in a supersonic flow of a dissociating gas [8–16, 47–49]. As is noted in Section 1, insofar as the dependence of the heterogeneous recombination probability on the state of the gas interacting with the surface has not been fully clarified, that method of investigation is selected which would provide a good fit of experimental conditions to the conditions of subsequent use in practice of the measured values of γ_w. Below, main errors and assumptions in the recovery of the value of heterogeneous recombination probability will be considered in brief.

For gas dissociation most common are glow and microwave discharges in the first group of methods, and powerful arc and superhigh frequency discharges in the second group. Erosion of electrodes in glow and arc discharges contaminates the surface of the studied specimen and alters the recombination activity in an uncontrollable way. A dissociating gas contains large quantities (up to 20%) of metastable particles, in particular singlet oxygen $1\Delta O_2$, and this may lead to an increasing heat flux [53] to the surface, and consequently, to the overestimation of the recovered values of γ_w [52]. In order to lower the amount of metastable particles in a dissociating gas it was suggested [52] to ballast mixtures with appreciable (about 70–90%) quantities of argon. It should be noted that metastable particles do not practically form in the thermal dissociation of gases.

The methods of the first group most frequently investigate a decrease of atom concentration along a reactive tube or some time after the end of the exciting pulse. Atoms perish as a result of homogeneous and heterogeneous recombination processes. For characteristic dimensions of reactors used and heterogeneous recombination probability $\gamma_w = 10^{-4}$–10^{-2} at pressures $P \lesssim 10^{-2}$ mmHg, the gas-phase recombination is not important [38, 46, 50, 51, 53]; when $P \lesssim 0.1$–0.5 mmHg, it can be taken into account as a correction for the main heterogeneous recombination process [37]. For high gas pressures $P \gtrsim 0.55$ mmHg, homogeneous and heterogeneous speeds of the death of atoms are commensurable. Therefore, under these conditions the recovery of γ_w is carried out either on the basis of other authors' data on the rate constants of homogeneous processes with participation of atomic oyxgen, or with the use of the methods which allow simultaneous recovery of the rate constants of homogeneous and heterogeneous death of atoms [37]. Note that uncertainties in the reaction rate constants of the homogeneous death of atoms may lead to appreciable errors in the recovery of the heterogeneous recombination probability which are most substantial at low values of $\gamma_w = 10^{-3}$–10^{-5} [37].

Other essential sources of errors include the distortion of the initial distribution of atomic concentration in a reactive vessel when a thermocouple is used for the recording of atoms. For materials with a low catalycity the death of atoms on the thermocouple may exert a substantial effect on the results of γ_w recovery [46]. Therefore, to obtain more reliable results, the content of atomic oxygen is determined by the ESR method, Wrede–Harteck gases [36], nitrogen oxide titration [36, 37], and by the optical diagnosis technique, which practically do not distort the original distribution of O atoms.

In absolute [48] and differential [47] calorimetric methods a major error in the γ_w recovery can be associated with uncertainty in the choice of the chemical energy accommodation coefficient β_w. The available few results on this coefficient for oxygen atom recombination, β_o, on different surfaces show that for many substances $\beta_{wo} \ll 1$. For a number of metals the value of β_{wo} for the surface temperature $T_w = 300$ K is shown to lie within 0.07–0.95 [53].

The chemical energy accommodation coefficient β_w may decrease as a result of the formation of excited particles in the course of surface recombination and their subsequent diffusion into the gas phase [54]. Thus, in absolute calorimetric methods, which are

Table 2. The measured hereogeneous recombination probabilities γ_w of oxygen atoms and experimental conditions of the present work

Material investigated	Initial gas pressure in a ST, P_1 (mmHg)	Incident SW velocity, u_s (mm μs^{-1})	Equilibrium parameters of a gas behind an incident SW						Gas parameters at the boundary-layer edge				
			Pressure, P_2 (mmHg)	Temperature, T_2 (K)	Flow velocity, u_2 (mm μs^{-1})	O–O_2–Ar mixture composition O (%)	O_2 (%)	Ar (%)	Pressure, P_e (mmHg)	Temperature, T_e (K)	Flow velocity, u_e (mm μs^{-1})	Heat flux to a surface Q_{wt} (cal $cm^{-2} c^{-1}$)	Heterogeneous recombination probability, γ_w
Platinum	0.96	2.99	118	3670	2.64	29	3	68	79	3180	2.76	40.0	1.0(−2)
	1.06	2.98	129	3670	2.63	29	3	68	90	3180	2.74	50.2	2.5(−2)
	0.96	3.07	125	3810	2.71	30	2	68	87	3300	2.83	42.0	1.0(−2)
	1.01	2.82	111	3460	2.48	25	5	70	78	3020	2.59	37.1	1.5(−2)
Alumina	0.96	3.03	121	3740	2.68	30	2	68	84	3240	2.80	33.0	2.5(−3)
	1.01	3.03	128	3740	2.68	30	2	68	89	3240	2.79	34.3	2.0(−3)
Silicon monoxide (SiO)	0.95	3.06	122	3790	2.70	30	2	68	85	3280	2.82	35.6	3.0(−3)
	1.08	3.06	139	3800	2.70	30	2	68	96	3290	2.82	37.1	2.0(−3)
	0.96	3.03	121	3740	2.68	30	2	68	84	3240	2.80	35.0	3.6(−3)
	1.01	3.07	131	3820	2.71	30	2	68	92	3310	2.83	36.8	2.8(−3)
	0.96	2.99	118	3670	2.64	30	2	68	82	3180	2.76	31.5	1.8(−3)

Figures in round brackets denote orders of magnitude.

Table 3. The measured probabilities of heterogenous recombination of oxygen atoms on quartz (SiO_2), silicon monoxide (SiO) oxidized in the O_2 atmosphere, platinum and alumina at the surface temperature T_w = 300–400 K and under the conditions of experiments

Material investigated	No.	Method of measurement	Method of gas excitation	Method of determining the concentration of atoms	Initial composition of mixture (mole %)
Experiment 1	2	3	4	5	6
Vycor (96% SiO_2)	1	continuous-flow reactor	MD*	luminosity of O/NO, λ = 5500 Å	O_2
	2	continuous-flow reactor	MD*	NO titration	O_2+3Ar
	3	side sleeve	MD*	thermocouple heating	O_2
	4	side sleeve	MD*	thermocouple heating	O_2
Fused quartz	5	continuous-flow reactor	MD*	ESR	O_2+100Ar
	6	continuous-flow reactor	high-frequency discharge	ESR	O_2+2.5He
	7	capillary heating in gas jet	glow discharge	Wrede–Harteck probe	O_2
	8	side sleeve	MD*	ESR	O_2
	9	by a decrease in concentration of atoms near specimen surface	MD*	thermocouple heating	O_2
SiO_2 monocrystal (0001) face	10	by a decrease in concentration of atoms near specimen surface	MD*	thermocouple heating	O_2
	11	side sleeve	MD*	thermocouple heating	O_2
	12	by heat flux to stagnation point	glow discharge	heat flux to ideally catalytic surface	air
			in shock tube with glow discharge	heat flux to ideally catalytic surface	air
			plasma generator discharge	heat flux to ideally catalytic surface	air
Silicon monoxide (vacuum deposition)	13	heat flux to stagnation point	plasma generator discharge	heat flux to ideally catalytic surface	air
	14	the difference of heat fluxes to the material investigated	MD*	NO titration	O_2
	15	heat flux to flat plate	thermal discharge behind shock wave	calculation	O_2+4Ar
	16	decrease of luminosity in reaction vessel	glow discharge	luminosity of O+NO	O_2+(4–8)Ar
	17	side sleeve	MD*	thermocouple heating	O_2
Alumina	18	see No. 14			
	19	difference of heat fluxes to the material investigated and noncatalytic surface	MD*	—	O+9Ar
	20	see No. 15			
	21	see No. 7			
	22	see No. 17			
Platinum	23	continuous-flow pipe with a specimen in its end	MD*	Wrede–Harteck probe	O_2
	24	see No. 14			
	25	see No. 13			
	26	see No. 15			

* MD = microwave discharge.

Content of atoms (mole %)	Gas pressure at the surface (mmHg)	Flow velocity ($m\ s^{-1}$)	Probability of heterogeneous recombination	Preparation and cleaning of the surface	Remark	Ref.
7	8	9	10	11	12	13
14	0.2–1.6	1–12	4.7(−5)	in hydrofluoric acid and distilled H_2O	—	[36]
0.2–4.0	4	0.5–1.0	2.7–7.8(−5)	in hydrofluoric and nitric acids and distilled H_2O	—	[37]
10–15	3(−2)	—	3.5(−4)	in chromic acid and distilled H_2O	—	[38]
1–25	0.08–0.15	—	7.1(−4)	acids and distilled H_2O	—	[39]
1	0.82–2.65	1.5–5.2	0.78–1.0(−4)	not given	—	[40]
—	0.5	—	6.1(−3)	in hydrofluoric acid and distilled H_2O	—	[41]
			1.7(−2)	KCl solutions		
30	0.1–0.2	0.5	2(−4)	not given	—	[42]
1	1–2	—	3.2(−4)	in nitric acid and distilled H_2O	—	[43]
20	0.2	—	1.4(−2)	etching in hydrofluoric acid, washing in distilled H_2O and alcohol	—	[44]
13	0.11	—	1.8(−4)	etching in nitric acid and washing in distilled H_2O	—	[45]
25	0.05	—	1.6(−4)	cleaning with acids	—	[46]
1–3	0.5	10	1.3(−4)	in acid and distilled H_2O	heat flux	[47]
			6.5(−4)	without additional cleaning	$Q_{wt} = 10^{-3}$ W cm^{-2}	
1.1	0.5	$M = 2.8$	3.2 + 1.3–1.9 (−3)	without additional cleaning	heat flux Wcm^{-2}	[48]
			3.2(−2)	kept for a week in air		
—	8.3	$M = 4.7$	3.2 + 1.3–1.9 (−3)	without additional cleaning	$Q_{wt} \approx 30$ W cm^{-2}	
—	1.5–5	—	1(−3)	not given	total enthalpy of flux $h_t = 8.2$–20 MJ kg^{-1}	[48]
0.66–5	0.1–1.0	15	1(−4)	holding in flow of dissociating O_2 for oxidizing	$Q_{wt} = 1.0$–1.7 W cm^{-2}	[49]
30	80–90	2600–2800	1.8–3.5(−3)	without additional cleaning	$Q_{wt} = 140$ W cm^{-2}	present work
1–2	10^{-5}	—	3.2(−3)	foil without additional treatment	—	[50]
			5(−2)	non-polished surface of (1100) face		
25	0.05–0.11	—	1.8–3.4(−3)	vacuum deposition. Heating in O_2 atmosphere for oxidizing	—	[51]
			2.1(−3)	aluminum pipe	—	[46]
			1(−2)	vacuum deposition and holding in the flow of dissociated O_2	—	[49]
1.3	5.7	4.0	6.8(−3)	vacuum deposition and holding in O_2 flow for oxidizing	—	[52]
			2.5(−3)	vacuum deposition and oxidizing by heating in O_2	$Q_{wt} = 130$ W cm^{-2}	present work
			4.0(−2)	cathode deposition	—	[42]
			0.55–4.9(−3)	vacuum deposition and oxidizing by heating in O_2 atmosphere	—	[51]
10–15	0.5–3.0(−2)	0–1.2	1.4–0.4(−2)	platinum wire 99.95%	chemical energy accommodation coefficient $\beta = 0.1$–0.4	[53]
			4–3(−3)	vacuum deposition and holding in dissociated O_2	—	[49]
			9.0(−2)	vacuum deposition	—	[48]
			1–2.5(−2)	fire-fitting from the solution of oil with alcohol	$Q_{wt} = 160$–200 W cm^{-2}	present work

based on the measurement of heat fluxes, the value of the product γ_w and β_w is virtually recovered which is the coefficient of energy transfer catalytic recombination. Therefore, the actual values turn out to be understated by a factor of about $1/\beta_w$ as compared with the data reported. In differential calorimetric methods the difference between the chemical energy accommodation coefficients, β_w, of the standard and investigated materials will also lead to errors in the recovery of heterogeneous recombination probability γ_w.

The data obtained in the present work on the heterogeneous recombination probability γ_w (actually of the energy transfer catalytic recombination coefficient as shown above) for hydrogen atoms on a vacuum deposited silicon monoxide thin film, oxidized thereafter in air, lies within $(1.8–35) \times 10^{-3}$ (Table 2). The values of γ_w for deposited and oxided films of SiO or SiO-based materials, obtained by other authors, vary within $10^{-4}–3.2 \times 10^{-2}$ (Table 3). Measurements by the side sleeve method for SiO surfaces cleaned with acids gave $\gamma_w = (1.6–1.8) \times 10^{-4}$ [45–47] (Table 3). The deposited SiO films were investigated by different methods [47]: with the use of a continuous flow reactor, in a supersonic flow behind a shock wave and at the exit from a supersonic nozzle of a plasma generator. The values of γ_w obtained in supersonic flow in a shock tube and in a plasma generator are about 25 times higher than the heterogeneous recombination probabilities determined with the use of a continuous flow reactor. The treatment of SiO_2 film with acids reduces

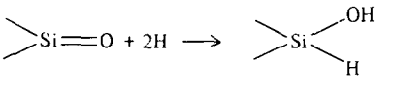

the values of γ_w, measured by these methods, by about 6–10 times.

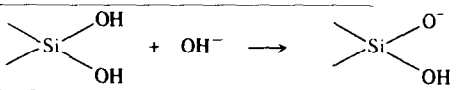

The heterogeneous recombination probability γ_w for fused quartz is somewhat lower than for oxidized SiO film and lies within the range $2.7 \times 10^{-5}–7.1 \times 10^{-4}$ [36–42]. For the (0001) face of a SiO_2 monocrystal the value of γ_w is about 1.4×10^{-2} [44]. The treatment of the fused quartz surface with alkali increases the catalytic activity by more than 2–3 times [41].

These decreases and increases of the catalytic activity on treatment of quartz with acids and alkali, respectively, can be explained within the framework of the theory [55] presuming that the recombination process follows the Rideal–Eley mechanism and that the active centers on the surface are represented by the groups

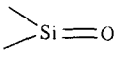

and

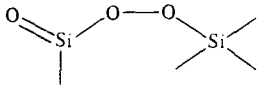

A low content of active centers on the quartz surface is responsible for a low recombination catalytic activity of the entire material. At low surface temperatures, $T \simeq 300$ K, the greater part of the active centers is filled with hydroxyl groups:

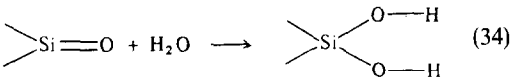

(34)

and

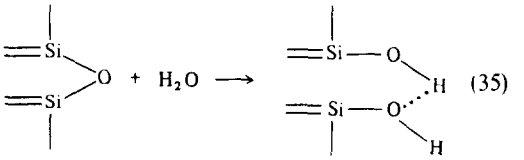

(35)

Note that the washing of the quartz surface is made at the final stage of surface cleaning (see Table 3). The treatment of the surface with acids also leads to lesser quantities of free active centers according to the mechanism [55]:

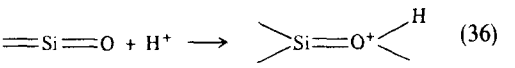

(36)

In a number of cases, in order to obtain a higher amount of monatomic oxygen in gas excitation by electric or microwave discharges, water vapor is added to the working medium. The recombination catalytic activity of quartz may decrease in this case during exposure due to the death of active centers [55]

(37)

and vice versa, when the quartz surface is treated with alkali the number of active centers increases

(38)

which leads to an increase of the recombination catalytic activity. The data of Table 2 illustrate the current uncertainty in the measured values of γ_w for quartz due to different experimental conditions and preparation of surfaces.

Note that the method developed in this work allows investigations at gas pressures of about 80–100 mmHg above surfaces (Table 3) which is 1.5–2 orders of magnitude higher than the upper limit for the pressures, $P \simeq 1–5$ mmHg, attained in previous studies (Table 3). Since the heterogeneous recombination mechanism may vary at different gas pressures, this extension of the range of investigation seems to be essential.

The heterogeneous recombination probabilities of oxygen atoms of alumina measured in studies [46, 50–52] and in this work, also with the use of different methods, are rather well correlated (Table 3). The value of γ_w in these studies for alumina changes within $(1.8–6.8) \times 10^{-3}$, with the majority of values for γ_w, obtained in these works, lying in a narrow range $\gamma_w = (1.8–3.4) \times 10^{-3}$. The results obtained in ref. [52] seem

to be an overestimate. The surfaces investigated in the above-mentioned studies differed markedly—from aluminium pipe in work [46] to vacuum deposition of aluminium film with subsequent oxidizing in the oxygen atmosphere in studies [49–52] and in this work. For a nonpolished (1100) face at pressures of $P \simeq 10^{-5}$ mmHg, much higher values of γ_w were obtained in work [50], i.e. $\gamma_w = 5 \times 10^{-2}$. Thus, in a wide range of gas pressures, $P = 10^{-5}$–100 mmHg, and concentrations of oxygen atoms, x_0, the heterogeneous recombination probability of O atoms on alumina constitutes $(1.8–6.8) \times 10^{-3}$.

The measured results on the catalytic activity of platinum can be divided into two groups (Table 3). The first group is characterized by low values of γ_w, i.e. $\gamma_w = (0.55–4.0) \times 10^{-3}$ [49, 51]. These results are obtained with the use of the side sleeve method and a continuous-flow reactor. For the second group, higher values of γ_w were obtained, i.e. $\gamma_w = (1.4–9.0) \times 10^{-2}$ [42, 48, 49, 53, and the present work]. These results were obtained with the use of different methods including supersonic blowing. Note that according to ref. [53] the coefficient of chemical energy accommodation with oxygen recombination on platinum is $\beta \simeq 0.1$. Therefore, according to the reasoning given above, the results on γ_w measured by the heat flux in [48, 49] and in the present work can be understated by about an order of magnitude. This further increases the scatter in the data on the catalytic activity factor for oxygen atoms on platinum obtained by different authors.

It should be noted that the lowest values of γ_w for platinum were obtained in the conditions when the surface was exposed to the attack of dissociated oxygen for a long time [49, 51]. It was shown [52] that at the initial instant of time a clean platinum film has a low catalytic activity which increases with exposition for about 250 μs up to steady-state values. With further exposition of platinum there occurs a certain decrease in the catalytic activity of its surface. Therefore it can be assumed that a decrease [49, 51] in recombination catalytic activity of platinum on prolonged attack of oxygen is associated with a change in the structure of its surface and with the formation of PtO oxides.

9. CONCLUDING REMARKS

In the present work, a pulsing method has been developed to determine the probability of heterogeneous recombination of materials from the measured heat fluxes to the surface of a wedge-like plate in a quasi-steady-state supersonic flow of a gas dissociated behind a shock wave. The method allows the recovery of the time-resolved values of heterogeneous recombination probability of materials and extends the range of gas pressures near the surface by two orders of magnitude up to 100 mmHg. The heterogeneous recombination probability of vacuum deposited and oxidized films of aluminium, silicon monoxide and platinum at the surface temperature of $T_w = 300$ K has been measured and comparison with the results of other authors has been made.

Acknowledgement—The authors wish to thank Professor V. L. Talrose for his constant attention to and interest in the present work.

REFERENCES

1. V. P. Agafonov, V. K. Vertushkin, A. A. Gladkov and O. Yu. Polyansky, *Non-equilibrium Physicochemical Processes in Aerodynamics*. Izd. Mashinostroenie, Moscow (1972).
2. S. Z. Roguinsky and A. Shekhter, On the recombination of atoms or oxygen and hydrogen on metals, *Dokl. Akad. Nauk SSSR* **1**, 310–312 (1934).
3. V. I. Goldansky, N. N. Semyonov and N. M. Chirkov, Heterogeneous catalysis in polymolecular adsorption layers, *Dokl. Akad. Nauk SSSR* **52**, 783–785 (1946).
4. V. V. Voyevodsky and G. K. Lavrovskaya, Recombination of atoms on solid surfaces, *Dokl. Akad. Nauk SSSR* **63**, 151–154 (1948).
5. E. B. Gordon, A. N. Ponomaryov and V. L. Talrose, The study of the probability of recombination of atomic hydrogen on different surfaces at low concentrations of atoms in gas phase, *Kinet. Katal.* **VII**, 577–582 (1966).
6. W. V. Smith, Surface recombination of H atoms and OH radicals, *J. chem. Phys.* **11**, 110–125 (1943).
7. V. A. Lavrenko, *Recombination of Hydrogen Atoms on Solid Body Surfaces*. Izd. Naukova Dumka, Kiev (1973).
8. D. E. Rosner, Diffusion and chemical surface catalysis in a low-temperature plasma jet, *Trans. Am. Soc. mech. Engrs*, Series C, *J. Heat Transfer* **84**, 386–394 (1962).
9. G. M. Prok, Nitrogen and oxygen atom recombination at oxide surfaces and effect of a tesla discharge on recombination heat transfer, NASA-Report, TND-1567, Washington (1963).
10. W. H. Carden, Experimental heat transfer to hemispheres in non-equilibrium dissociated hypersonic flow with surface catalysis and second order effects, AIAA-paper, N 66-3 (1966).
11. L. A. Anderson, Effect of surface catalytic activity on stagnation heat transfer rates, *AIAA Jl* **11**, 649–656 (1973).
12. E. B. Zhestkov and A. Ya. Knivel, Some aspects of non-equilibrium free molecular nitrogen flow-metal surface interaction. In *Proc. 13th Int. Symposium on Rarefied Gas Dynamics*, Inst. of Thermophysics, Book of Abstracts vol. 1, pp. 141–142, Novosibirsk (1982).
13. A. N. Gordeyev, A. F. Kolesnikov and M. I. Yakushin, Investigation of heat transfer on models in subsonic jets of an induction plasma generator, *Mekh. Zhidk. Gaza* **6**, 129–135 (1983).
14. R. I. Soloukhin, Measurement of the rate of oxygen recombination in shock waves, *Fiz. Gor. Vzryva* **3**, 402–410 (1965).
15. A. E. M. Nasser and R. A. East, A shock tube investigation of heat transfer from dissociated hydrogen to catalytic surfaces, *Int. J. Heat Mass Transfer* **23**, 515–526 (1980).
16. V. M. Doroshenko, N. N. Kudryavtsev, S. S. Novikov and A. I. Sharovatov, The laboratory method of measuring the catalytic activity of heated bodies. In *Elementary Processes in Chemically Reacting Media (Collected Papers)*, pp. 58–65. Izd. MFTI (1983).
17. R. J. Vidal and T. C. Golian, Heat-transfer measurements with a catalytic flat plate in dissociated oxygen, *AIAA Jl* **5**, 1579–1587 (1967).
18. P. M. Chung, Chemically reacting non-equilibrium boundary layer. In *Advances in Heat Transfer*, Vol. 11, pp. 109–270. Academic Press, New York (1965).

19. H. Mirels and S. W. King, Series solutions for shock-tube laminar boundary layer and test time, *AIAA Jl* **4,** 621–628 (1966).
20. D. Sharma and L. Wray, Excitation mechanism for the O_2 Shuman–Runge system, *J. chem. Phys.* **54,** 4578–4584 (1971).
21. M. Camac and A. Vaughn, O_2 dissociation rates in O_2–Ar mixtures, *J. chem. Phys.* **34,** 460–470 (1961).
22. C. H. Lewis and E. W. Miner, Hypersonic ionizing air viscous shock-layer flows over nonanalytic blunt bodies, NASA-Report CR-2550, Washington (1975).
23. A. Yu. Zakharov and V. I. Turchaninov, STIFF program for the solution of rigid systems of ordinary differential equations. Preprint of the Institute of Applied Mechanics of the USSR Academy of Sciences, Moscow (1977).
24. T. V. Bazhenova, L. G. Gvozdyova, Yu. S. Lobastov, I. M. Naboko, R. G. Nemkov and O. A. Predvoditelev, *Shock Waves in Real Gases.* Izd. Nauka, Moscow (1968).
25. H. W. Liepmann and A. Roshko, *Elements of Gas Dynamics.* John Wiley, New York (1957).
26. W. H. Dorrance, *Viscous Hypersonic Flow.* McGraw-Hill, New York (1962).
27. G. A. Tirsky, Calculation of the effective coefficients of diffusion in a laminar dissociated multicomponent boundary layer, *Prikl. Mat. Mekh.* **33,** 180–192 (1969).
28. I. V. Petukhov, On the realization of the two-step difference scheme for boundary layer equations, Trudy TsAGI No. 1582, pp. 3–7 (1974).
29. P. L. Chambre and A. Acrivos, On chemical surface reactions in laminar boundary-layer flows, *J. appl. Phys.* **27,** 1323–1328 (1956).
30. T. Y. Li and P. S. Kirk, Asymptotic method of solution of the frozen dissociated laminar boundary-layer flow over a flat-plate surface with arbitrarily distributed catalycity, *Int. J. Heat Mass Transfer* **10,** 257–266 (1967).
31. A. Takano, Integral method of solution for non-equilibrium boundary layer flow of a dissociated gas over a catalytic flat plate, *Trans. Jap. Soc. Aerospace Sci.* **13,** 10–26 (1970).
32. M. A. Van Dyke, Review and extension of second-order hypersonic boundary-layer theory. In *Rarefied Gas Dynamics* (edited by J. A. Laurmann), Vol. 11, pp. 212–227. Academic Press, New York (1963).
33. R. Goulard, On catalytic recombination rates in hypersonic stagnation heat transfer, *Jet Propul.* **28,** 733–745 (1958).
34. G. T. Skinner, Analog network to convert surface temperature to heat flux, *Am. Rocket Soc. J.* **30,** 569–570 (1960).
35. Yu. A. Polyakov and E. A. Mitkina, Thin film thermometer of resistance, *Priborȳ Tekh. Éksp.* No. 14, 140–143 (1961).
36. F. Kaufman, Reactions of oxygen atoms. In *Progress in Reaction Kinetics,* Vol. 1, pp. 1–39 (1961).
37. J. Berkowitz, Catalytic oxygen atom recombination on solid surfaces. Paper No. 80 in *The Structure and Chemistry of Solid Surfaces.* J. Wiley, New York (1969).
38. P. C. Dickens and M. B. Sutchiffe, Reactions of oxygen atoms on oxide surfaces, activation energy of recombination, *Trans. Farad. Soc.* **60,** 1272–1285 (1964).
39. J. W. Linnett and D. G. H. Marden, The kinetics of the recombination of oxygen atoms at a glass surface, *Proc. R. Soc.* **234,** 489–504 (1956).
40. V. V. Azatyan, F. A. Grigoryan and S. B. Filippov, Investigation of heterogeneous recombination of hydrogen and oxygen atoms by the EPMR method, *Kinet. Katal.* **13,** 1389–1392 (1972).
41. G. I. Ksandopulo, Z. A. Mansurov, A. S. Masalimov, S. P. Novikov and A. A. Saguindykov, Recombination of hydrogen and oxygen atoms on quartz surface. In *Chemistry and Chemical Engineering,* pp. 133–135. Izd. Kaz. GU, Alma-Ata (1979).
42. V. V. Voyevodsky and G. K. Lavrovskaya, Recombination of hydrogen and oxygen atoms on solid surfaces, *Zh. Fiz. Khim.* **25,** 1050–1057 (1959).
43. S. Krongelb and M. W. P. Strandberg, Use of paramagnetic resonance techniques in the study of atomic oxygen recombination, *J. chem. Phys.* **31,** 1196–1210 (1959).
44. V. A. Lavrenko, A. A. Chekhovsky and V. L. Tikush, Temperature dependence of the coefficient of recombination of atoms of hydrogen, oxygen and nitrogen on the surface of magnesium and silicon oxide monocrystals, *Kinet. Katal.* **15,** 1072–1075 (1974).
45. J. C. Greaves and J. W. Linnett, Recombination of atoms at surfaces. 6. Recombination of oxygen atoms at silica from 20 to 600°C, *Trans. Farad. Soc.* **55,** 1355–1361 (1959).
46. J. C. Greaves and J. W. Linnett, Recombination of atoms at surfaces. 5. Oxygen atoms at oxide surfaces, *Trans. Farad. Soc.* **55,** 1346–1354 (1959).
47. K. E. Starner and W. P. Thomson, Arc-tunnel studies of nonequilibrium stagnation point heat transfer. *Proc.* 1966 *Heat Transfer and Fluid. Mech. Inst.,* pp. 428–444. Stanford University Press, Stanford, California (1966).
48. L. A. Anderson, Effect of surface catalytic activity in stagnation heat transfer rates, *AIAA Jl* **11,** 649–656 (1973).
49. R. A. Hartunian, W. P. Thomson and S. Sabron, Measurements of catalytic efficiency of silver for oxygen atoms and the O–O_2 diffusion coefficient, *J. chem. Phys.* **43,** 4003–4006 (1965).
50. K. Loomis, R. R. Borgehdahl, R. R. Reeves and P. Harteck, Catalytic recombination of oxygen atoms at metal surfaces in the 10^{4}–10^{-6} torr pressure range, *J. Am. chem. Soc.* **91,** 7709–7712 (1969).
51. J. C. Greaves and J. W. Linnett, The recombination of oxygen atoms at surfaces, *Trans. Farad. Soc.* **54,** 1323–1330 (1958).
52. A. L. Myerson, Exposure-dependent surface recombination efficiencies of atom oxygen, *J. chem. Phys.* **50,** 1228–1234 (1969).
53. G. A. Melin and R. J. Madix, Energy accommodation during oxygen atom recombination at metal surfaces, *Trans. Farad. Soc.* **67,** 198–211 (1971).
54. P. Harteck, R. Reeves and G. Manela, Surface-catalyzed atom, *J. Chem.* **38,** 1648–1651 (1960).
55. M. Green, K. R. Lennings, J. W. Linnett and D. Schofied, Recombination atoms at surfaces. 7. Hydrogen atoms at silica and other similar surfaces, *Trans. Farad. Soc.* **55,** 2152–2161 (1959).
56. S. J. Gubley and E. A. Mason, Atom–molecule and molecule–molecule potentials and transport collision integrals for high-temperature air species, *Phys. Fluids* **18,** 1109–1111 (1975).
57. J. Hilsenrath (editor), *Tables of Thermodynamic and Transport Properties.* Pergamon Press, New York (1960).
58. C. R. Wilkie, A viscosity equation for gas mixtures, *J. chem. Phys.* 517–519 (1950).
59. J. O. Hirschfelder, C. F. Curtiss and R. B. Bird, *Molecular Theory of Gases and Liquids.* John Wiley, New York (1954).
60. L. Monchik, Collision integrals for the exponential repulsive potential, *Phys. Fluids* **2,** 695–700 (1959).
61. E. A. Mason and S. C. Saxena, Approximate formula for the thermal conductivity of gas mixtures, *Phys. Fluids* **1,** 361–369 (1958).

APPENDIX: CALCULATION OF TRANSPORT COEFFICIENTS

The calculation of the transport properties of the O–O_2–Ar gas mixture species, i.e. viscosity μ_i, thermal conductivity λ_i, and the coefficient of binary diffusion at high temperatures $T \geqslant 2000$ K was carried out with the use of experimental potentials of interaction [56]. The determination of these

parameters for the conditions on a cold wall ($T_w = 300$ K) was carried out on the basis of the available experimental measurements of the values of μ_i, λ_i and D_{ik} [57].

For the determination of the gas mixture viscosity the following relation was used [58]

$$\mu = \sum_i \mu_i \left(1 + \sum_{i \neq k} G_{ik} \frac{x_k}{x_i}\right)^{-1} \tag{A1}$$

where x_i and x_k are the mole fractions of i and k species

$$G_{ik} = \left[1 + \left(\frac{\mu_i}{\mu_k}\right)^{1/2} \left(\frac{m_k}{m_i}\right)^{1/4}\right]^2 \left[2\sqrt{2}\left(1 + \frac{m_i}{m_k}\right)^{1/2}\right]. \tag{A2}$$

The partial viscosities of the mixture species μ_i at high temperatures were calculated as [59]

$$\mu_i = 266.93 \times 10^{-7} \frac{(m_i T)^{1/2}}{\sigma_{ii}^2 \Omega_{ii}^{(2,2)*}} \text{ g cm}^{-2} \text{ s}^{-1} \tag{A3}$$

where σ_{ii} are the collision diameters (Å) [56], $\Omega_{ii}^{(2,2)*}$ the reduced collision integrals tabulated at different energies of interaction [60]. The quantity $\Omega_{ii}^{(2,2)*}$ was calculated with the use of the parameters of exponential interaction potential [56].

The thermal conductivity of a gas mixture was determined by the relation [61]

$$\lambda = \sum_i \lambda_i \left(1 + 1.065 \sum_{i \neq k} G_{ik} \frac{x_k}{x_i}\right)^{-1}. \tag{A4}$$

The values of λ_i at high temperatures were calculated as [59]

$$\lambda_i = \frac{15}{4} \frac{R}{m_i} \cdot \mu_i \left(0.115 + 0.354 \frac{C_{pi} m_i}{R}\right). \tag{A5}$$

The binary diffusion coefficients D_{ik} were calculated from [59]:

$$D_{ik} = 262.8 \times 10^{-5} \frac{[T^3 (m_i + m_k)/2 m_i m_k]^{1/2}}{P \cdot \sigma_{ik}^2 \Omega_{ik}^{(1,1)*}} \text{ cm}^2 \text{ s}^{-1}$$

where $\Omega_{ik}^{(1,1)*}$ is the reduced collision integral tabulated at different energies of interaction [59], P is the gas pressure (atm.). In an analogous way, to calculate the value of $\Omega_{ik}^{(1,1)*}$ the parameters of the exponential interaction potential [56] were used.

DETERMINATION DES PROBABILITES RESOLUES EN TEMPS DE LA RECOMBINAISON HETEROGENE D'ATOMES DANS UN TUBE A CHOC EXPERIMENTAL

Résumé—Une technique expérimentale est exploitée pour mesurer des probabilités résolues en temps de recombinaison hétérogène en surface d'atomes sur une plaque avec un bord d'attaque effilé, exposé à un écoulement pulsé supersonique de gaz dissocié par une onde de choc incidente dans un tube à choc. On suggère une méthode pour calculer le transfert thermique à la surface de la plaque pour les conditions expérimentales. On développe la conception d'une jauge à flux thermique et la technique de fabrication.

BESTIMMUNG DER ZEITABHÄNGIGEN WAHRSCHEINLICHKEIT EINER HETEROGENEN ATOMREKOMBINATION BEI STOSSROHRVERSUCHEN

Zusammenfassung—Ein Verfahren zur Messung der zeitabhängigen Wahrscheinlichkeit einer heterogenen Oberflächenrekombination von Atomen wurde entwickelt und experimentell an einer Platte mit einer scharfen Vorderkante durchgeführt, die von einem pulsierenden Überschallgasstrom umströmt wurde. Das Gas wurde durch eine einfallende Druckwelle, die sich in einem Stoßrohr ausbreiten konnte, dissoziiert. Eine Methode, um den Wärmeübergang an der Plattenoberfläche bei den vorliegenden Versuchsbedingungen abzuschätzen, wird mitgeteilt. Der Entwurf eines Wärmestromdichte-Meßgeräts und die Technologie seiner Herstellung wurden ausgearbeitet.

ОПРЕДЕЛЕНИЕ МГНОВЕННЫХ ЗНАЧЕНИЙ ВЕРОЯТНОСТИ ГЕТЕРОГЕННОЙ РЕКОМБИНАЦИИ АТОМОВ В ЭКСПЕРИМЕНТАХ НА УДАРНЫХ ТРУБАХ

Аннотация—Экспериментально реализован метод измерения мгновенных значений вероятности гетерогенной рекомбинации атомов на поверхностях при импульсном обдуве пластины с острой передней кромкой сверхзвуковым потоком газа, диссоциированного падающей ударной волной, распространяющейся в ударной трубе. Разработан метод расчета тепловых потоков на поверхности пластины в условиях эксперимента. Разработана конструкция датчика теплового потока и технология ее изготовления.